NATIONAL INSTITUTE FOR FUSION SCIENCE

Quantum Nernst Effect

H. Nakamura, N. Hatano and R. Shirasaki

Quantum Nernst Effect

Hiroaki Nakamura[1]*, Naomichi Hatano[2], and Ryōen Shirasaki[3]

[1] *Theory and Computer Simulation Center, National Institute for Fusion Science, Oroshi-cho 322-6, Toki, Gifu 509-5292*
[2] *Institute of Industrial Science, University of Tokyo, Komaba 4-6-1, Meguro, Tokyo 153-8505*
[3] *Department of Physics, Yokohama National University, Tokiwadai 79-5, Hodogaya-ku, Yokohama 240-8501*

It is theoretically predicted for the two-dimensional electron gas that the Nernst coefficient is strongly suppressed and the thermal conductance is quantized in the quantum Hall regime. The Nernst effect is the induction of a thermomagnetic electromotive force in the y direction under a temperature bias in the x direction and a magnetic field in the z direction. The quantum nature of the Nernst effect is analyzed with the use of edge currents and demonstrated numerically.

KEYWORDS: Nernst effect, Nernst coefficient, edge current, quantum Hall effect, thermoelectric power, thermomagnetic effect

Introduction: The (adiabatic) Nernst effect in a bar of conductor is the generation of a voltage difference in the y direction under a magnetic field in the z direction and a temperature bias in the x direction (Fig. 1). Each of the left and right ends of a conductor is attached to a heat bath with a different temperature, T_1 at the left end and T_2 at the right end. An insulator is inserted in between the conductor and each heat bath, so that only the heat transfer takes place at both ends. A constant magnetic field B is applied in the z direction. (In what follows, we always put $T_1 > T_2$ and $B > 0$.) Then the Nernst voltage V_N is generated in the y direction.

A classical mechanical consideration on this thermomagnetic effect yields the following: a heat current flows from the left end to the right end because of the temperature bias; the electrons that carry the heat current receive the Lorentz force from the magnetic field and deviate to the upper edge; then we have $V_N < 0$. The Nernst coefficient is defined as

$$N \equiv \frac{V_N/W}{B\nabla_x T}, \qquad (1)$$

where the temperature gradient is given by $\nabla_x T = -(T_1 - T_2)/L$ with W and L being the width and the length of the conductor bar. The above naive consideration gives a positive Nernst coefficient. In reality, the Nernst coefficient can be positive or negative, depending on the scattering process of electrons.

The Nernst effect was extensively investigated in the 1960's[1] because of a possible application to conversion of heat to electric energy. The investigation on the energy conversion was eventually abandoned, since induction of the magnetic field cost lots of energy in those days. The Nernst effect, however, has recently seen renewed interest;[2-4] improvement of the superconducting magnet has led to more efficient induction of a strong magnetic field. This is a background of recent studies on the Nernst effect at temperatures higher than the room temperature.

In the present paper, we direct our attention to the Nernst effect in the quantum Hall regime, that is, the Nernst effect of the two-dimensional electron gas in semiconductor heterojunctions at low temperatures, low enough for the mean free path to be greater than the system size. Using a simple argument with edge currents,[5] we predict that, when the chemical potential is located between a pair of Landau levels, (i) the Nernst coefficient is strongly suppressed and (ii) the thermal conductance in the x direction is quantized.

Predictions: Let us first briefly explain our basic idea (Fig. 2). Since there is no input or output electric current I_e, an edge current circulates around the Hall bar when the chemical potential is in between neighboring Landau levels. The edge current along the left end of the
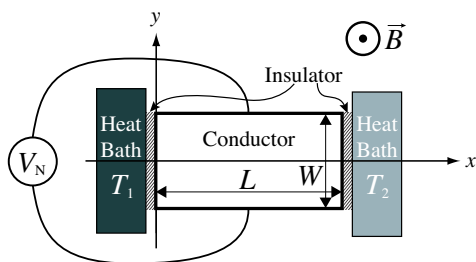

Fig. 1. A setup for observation of the (adiabatic) Nernst effect. The Nernst voltage V_N is defined as such that it is positive when the voltage of the upper edge is higher than the voltage of the lower edge.
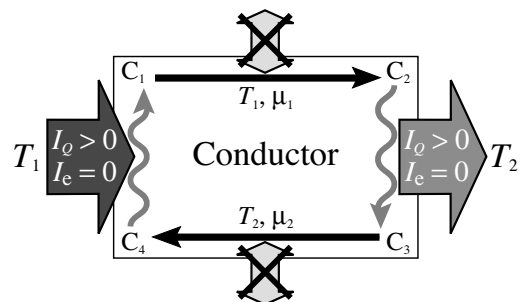

Fig. 2. A schematic view of the dynamics of electrons in a Hall bar under the setup for the Nernst effect.

*E-mail address: nakamura@tcsc.nifs.ac.jp

Hall bar is in contact with the heat bath with the temperature T_1 and equilibrated to the Fermi distribution $f(T_1, \mu_1)$ with the temperature T_1 and a chemical potential μ_1 while running from the corner C_4 to the corner C_1. Since the upper edge is not in contact with anything, the upper edge current runs ballistically, maintaining the Fermi distribution $f(T_1, \mu_1)$ all the way from the corner C_1 to the corner C_2. It then encounters the other heat bath with the temperature T_2 and equilibrated to the Fermi distribution $f(T_2, \mu_2)$ while running from the corner C_2 to the corner C_3. The lower edge current runs ballistically likewise, maintaining the Fermi distribution $f(T_2, \mu_2)$ all the way from the corner C_3 to the corner C_4. The Nernst voltage $V_N = \Delta\mu/e$ is thus generated, where $\Delta\mu \equiv \mu_1 - \mu_2$ and $e (< 0)$ denotes the charge of the electron.

First, the difference in the chemical potential, $\Delta\mu$, is of a higher order of the temperature bias $\Delta T \equiv T_1 - T_2$, because the number of the conduction electrons is conserved. The Nernst coefficient (1), or

$$N = \frac{1}{|e|B} \frac{L}{W} \frac{\Delta\mu}{\Delta T}, \quad (2)$$

hence vanishes as a linear response. Second, the heat current I_Q in the x direction is carried ballistically by the upper and lower edge currents. The edge currents do not change much when we vary the magnetic field as long as the chemical potential stays between a pair of neighboring Landau levels. The heat current hence has quantized steps as a function of the magnetic field.

Two-dimensional electron gas: We now describe the above idea explicitly. In order to fix the notations, we begin with the basics of the two-dimensional electron gas in a magnetic field. The dynamics of the two-dimensional electron gas is described by the Schrödinger equation

$$\left[\frac{(p_x + eBy)^2}{2m} + \frac{p_y^2}{2m} + V(y) \right] \Psi(x, y) = E\Psi(x, y), \quad (3)$$

where the energy is measured from the subband of the confining potential in the z direction. The potential $V(y)$ is the confining potential in the y direction, shown schematically in Fig. 3. We can express the eigenfunction of eq. (3) in the form of variable separation: $\Psi(x, y) = e^{ikx}\chi_k(y)/\sqrt{L}$, where $k = 2\pi j/L$ with an integer j. The transverse part $\chi_k(y)$ is an eigenfunction of the equation $\mathcal{H}_k\chi_k(y) = E\chi_k(y)$, where the Hamiltonian is given by

$$\mathcal{H}_k \equiv \frac{p_y^2}{2m} + \frac{m\omega_c^2}{2}(y - y_k)^2 + V(y) \quad (4)$$

with $\omega_c \equiv |e|B/m$ and $y_k \equiv \hbar k/(|e|B)$. The solutions are discrete and we label them with an integer n. After all, the whole solution is given by $\Psi_{n,k}(x, y) = e^{ikx}\chi_{n,k}(y)/\sqrt{L}$ with an eigenvalue $E = E(n, k)$. As is schematically shown in Fig. 3, the eigenvalue $E(n, k)$ in fact scarcely depends on k in the bulk, where the confining potential $V(y)$ is flat.[5, 6]

The Hamiltonian (4) shows that an eigenfunction with the x component of the momentum, $\hbar k$, is centered around $y = y_k \propto k$. In other words, the state in the
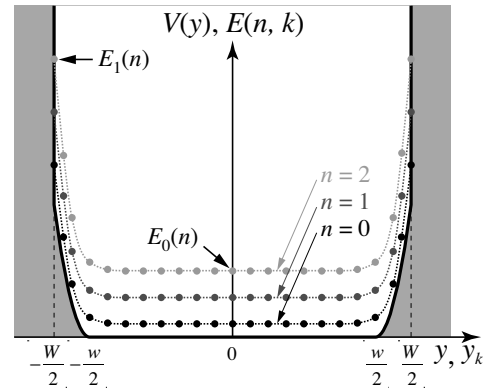

Fig. 3. A schematic view of the transverse confining potential $V(y)$, on which the structure of the Landau levels is superimposed. The central part of the potential, $|y| < w/2$, is flat, whereas the potential edges $w/2 < |y| < W/2$ may have some curvatures.

upper half of the Hall bar has a current in the positive x direction, while the one in the lower half has a current in the negative x direction. The velocity of the electron in the state $\Psi_{n,k}$ is

$$v(n, k) = \frac{1}{\hbar} \frac{\partial E(n, k)}{\partial k}, \quad (5)$$

which remains finite only near the upper and lower edges. These are the edge currents.

Electric and heat currents: Now we write down the electric current I_e and the heat current I_Q in the x direction carried by electrons. (Note that we will put $I_e = 0$ in the bottom line, observing the boundary conditions in Fig. 2.) The currents are given by

$$\begin{aligned} I_e &= \frac{1}{L} \sum_{n=0}^{\infty} \sum_{k, \uparrow\downarrow} ev(n, k) f_{n,k}(T(y_k), \mu(y_k)) \\ &= \frac{e}{\pi} \sum_{n=0}^{\infty} \int_{-k_m}^{k_m} v(n, k) f_{n,k}(T(y_k), \mu(y_k)) \, dk, (6) \end{aligned}$$

$$\begin{aligned} I_Q &= \frac{1}{\pi} \sum_{n=0}^{\infty} \int_{-k_m}^{k_m} (E(n, k) - \mu) \times \\ &\qquad v(n, k) f_{n,k}(T(y_k), \mu(y_k)) \, dk, (7) \end{aligned}$$

where we made the summation over k to the momentum integration. The upper and lower limits of the integration, $\pm k_m$, are the maximum and minimum possible momenta. The function $f_{n,k}$ denotes the Fermi distribution $f(T, \mu) = \{1 + \exp[(E - \mu)/(k_B T)]\}^{-1}$ with $E = E(n, k)$. Because of the layout in Fig. 2, the temperature $T(y_k)$ and the chemical potential $\mu(y_k)$ are T_1 and μ_1 for the upper edge states and T_2 and μ_2 for the lower edge states.

We transform eq. (6) with the use of eq. (5) as

$$\begin{aligned} I_e &= \frac{e}{\pi} \sum_{n=0}^{\infty} \Bigg[\int_{\text{upper}} v(n, k) f_{n,k}(T_1, \mu_1) \, dk \\ &\qquad + \int_{\text{lower}} v(n, k) f_{n,k}(T_2, \mu_2) \, dk \Bigg], \end{aligned}$$

$$= \frac{e}{\pi\hbar} \sum_{n=0}^{\infty} \int_{E_0(n)}^{E_1(n)} [f(T_1, \mu_1) - f(T_2, \mu_2)] \, dE. \quad (8)$$

Here $\int_{\mathrm{upper}}$ and $\int_{\mathrm{lower}}$ denote the integrations with respect to the upper and lower edge states, respectively. The lower limit of the energy integration is $E_0(n) = E(n, 0)$, while the upper limit is $E_1(n) = E(n, k_{\mathrm{m}})$ (see Fig. 3).

In order to compute the linear response, we here put $T_1 = T + \Delta T/2$, $T_2 = T - \Delta T/2$, $\mu_1 = \mu + \Delta\mu/2$, and $\mu_2 = \mu - \Delta\mu/2$, with $\Delta T \ll T$ and $\Delta\mu \ll \mu$. By expanding eq. (8) with respect to ΔT and $\Delta\mu$, we have

$$I_{\mathrm{e}} \simeq \frac{e}{\pi\hbar} \sum_{n=0}^{\infty} \int_{E_0(n)}^{E_1(n)} \left(\frac{\partial f}{\partial\mu} \Delta\mu + \frac{\partial f}{\partial T} \Delta T \right) dE$$

$$= \frac{e}{\pi\hbar} \left[\Delta\mu \sum_{n=0}^{\infty} A_0(n) + k_{\mathrm{B}} \Delta T \sum_{n=0}^{\infty} A_1(n) \right], \quad (9)$$

and similarly

$$I_Q \simeq \frac{k_{\mathrm{B}} T}{\pi\hbar} \left[\Delta\mu \sum_{n=0}^{\infty} A_1(n) + k_{\mathrm{B}} \Delta T \sum_{n=0}^{\infty} A_2(n) \right], \quad (10)$$

where

$$A_\nu(n) \equiv \int_{x_0(n)}^{x_1(n)} \frac{x^\nu \, dx}{4\cosh^2(x/2)} \quad (11)$$

with $x_i(n) \equiv (E_i(n) - \mu)/(k_{\mathrm{B}} T)$. The integral (11) can be carried out explicitly as

$$A_0(n) = \left[\frac{1}{2} \tanh \frac{x}{2} \right]_{x=x_0(n)}^{x_1(n)}, \quad (12)$$

$$A_1(n) = \left[\frac{x}{2} \tanh \frac{x}{2} - \log\cosh \frac{x}{2} \right]_{x=x_0(n)}^{x_1(n)}, \quad (13)$$

$$A_2(n) = \left[2\mathrm{Li}_2\left(-e^{-x} \right) - 2x \log\left(1 + e^{-x} \right) \right.$$
$$\left. - \frac{x^2}{2} \left(1 - \tanh \frac{x}{2} \right) \right]_{x=x_0(n)}^{x_1(n)}, \quad (14)$$

where $\mathrm{Li}_n(z) = \sum_{m=1}^{\infty} z^m/m^n$ is the polylogarithmic function.

Since there is no input or output current in the setup in Fig. 1, we put $I_{\mathrm{e}} \equiv 0$, relating $\Delta\mu$ with ΔT as

$$\Delta\mu = -\frac{\sum_n A_1(n)}{\sum_n A_0(n)} k_{\mathrm{B}} \Delta T. \quad (15)$$

We thereby arrive at the adiabatic Nernst coefficient eq. (2) in the form

$$N = -\frac{k_{\mathrm{B}}}{|e|B} \frac{L}{W} \frac{\sum_n A_1(n)}{\sum_n A_0(n)}. \quad (16)$$

The heat current (10) and eq. (15) yields the thermal conductance G_Q in the form

$$G_Q \equiv \frac{I_Q}{\Delta T} = \frac{k_{\mathrm{B}}^2 T}{\pi\hbar} \left[\sum_n A_2(n) - \frac{(\sum_n A_1(n))^2}{\sum_n A_0(n)} \right]. \quad (17)$$

Low-temperature limit: In the low-temperature limit, the upper and lower limits of the integration in eq. (11) goes to $\pm\infty$, depending on their signs. First, in the

usual experimental situation, the confining potential at its edges (of the order of eV) is considerably higher than the chemical potential (of the order of meV); hence we assume $E_1(n) > \mu$ for all n. The upper integration limit $x_1(n)$ thus always goes to $+\infty$ as $T \to 0$. Next, suppose that the chemical potential is located in between the bottom of the Mth Landau level and the bottom of the $(M+1)$th one. The lower integration limit $x_0(n)$ goes to $+\infty$ for $n \geq M + 1$ and the integration vanishes as $T \to 0$. The integration can survive only for $n \leq M$, for which the lower integration limit $x_0(n)$ goes to $-\infty$ as $T \to 0$, yielding $A_0(n) = 1$, $A_1(n) = 0$, and $A_2(n) = \pi^2/3$. (The integration A_ν for odd ν vanishes as the integrand is an odd function.) Thus we arrive at the predictions

$$N = 0 \quad \text{and} \quad \frac{G_Q}{T} = \frac{\pi k_{\mathrm{B}}^2}{\hbar} \frac{(M+1)}{3} \quad (18)$$

when the chemical potential is located in between the bottoms of a pair of the neighboring Landau levels.

Numerical demonstration: Let us demonstrate the quantum Nernst effect by adopting the following confining potential:[7]

$$V(y) = \begin{cases} 0 & \text{for} \quad |y| \leq \frac{w}{2}, \\ \frac{m\omega_0^2}{2} \left(|y| - \frac{w}{2} \right)^2 & \text{for} \quad \frac{w}{2} < |y| < \frac{W}{2}. \end{cases} \quad (19)$$

The parabolic parts near the edges cause a shift of the center of $\chi_k(y)$ from y_k to $Y_k \equiv (\omega_{\mathrm{c}}^2 y_k + \omega_0^2 w/2)/\omega_{\mathrm{c}0}^2$. The upper limit of the momentum integration is then given by $Y_{k_{\mathrm{m}}} = W/2$. The eigenvalues are well approximated in each region by tentatively regarding that the potential there continues for all y.[5] This gives[8–10]

$$E(n, k) \simeq \begin{cases} \left(n + \frac{1}{2} \right) \hbar\omega_{\mathrm{c}} & \text{for} \quad |y_k| \leq \frac{w}{2}, \\ \left(n + \frac{1}{2} \right) \hbar\omega_{\mathrm{c}0} + \left(\frac{\omega_{\mathrm{c}0}}{\omega_{\mathrm{c}}} \right)^2 \frac{m\omega_0^2(|Y_k| - w/2)^2}{2} & \\ \quad \text{for} \quad \frac{w}{2} < |y_k| < \frac{W}{2}, \end{cases} \quad (20)$$

where $\omega_{\mathrm{c}0} \equiv \sqrt{\omega_{\mathrm{c}}^2 + \omega_0^2}$. This approximation is valid because, in the parameter range that we use below, the width of the eigenfunction $\chi_{n,k}(y)$ for low n is much less than w, W and $W - w$; that is, each eigenfunction is well localized in the y direction and insensitive to the potential elsewhere. The mismatch of the approximated eigenvalue (20) at $|y| = w/2$ is much smaller than the eigenvalue itself because $\omega_0 \ll \omega_{\mathrm{c}}$ in the parameter range below.[7] Furthermore, the eigenvalue is shifted to[6]

$$E(n, k_{\mathrm{m}}) \simeq \left[(2n+1) + \frac{1}{2} \right] \hbar\omega_{\mathrm{c}0} + \left(\frac{\omega_{\mathrm{c}0}}{\omega_{\mathrm{c}}} \right)^2 \frac{m\omega_0^2(W-w)^2}{8} \quad (21)$$

right on the edges. This shift contributes only to a shift of $x_1(n)$, which is in fact irrelevant because $x_1(n)$ is virtually infinite anyway.

We set the parameters as follows: the effective mass is $m = 0.067 m_0$ for GaAs, where m_0 is the bare mass of the electron. The sample size is $L = 20\mu m$ and $W = 20\mu m$ (less than the mean free path at low temperatures[11]) with $w = 16\mu m$. The confining potential is given by $V(\pm W/2) = 5.0\mathrm{eV}$, the work function of GaAs. The chemical potential is $\mu = 15\mathrm{meV}$, which means the carrier density $n_{\mathrm{s}} = 4.24 \times 10^{15} \mathrm{m}^{-2}$.
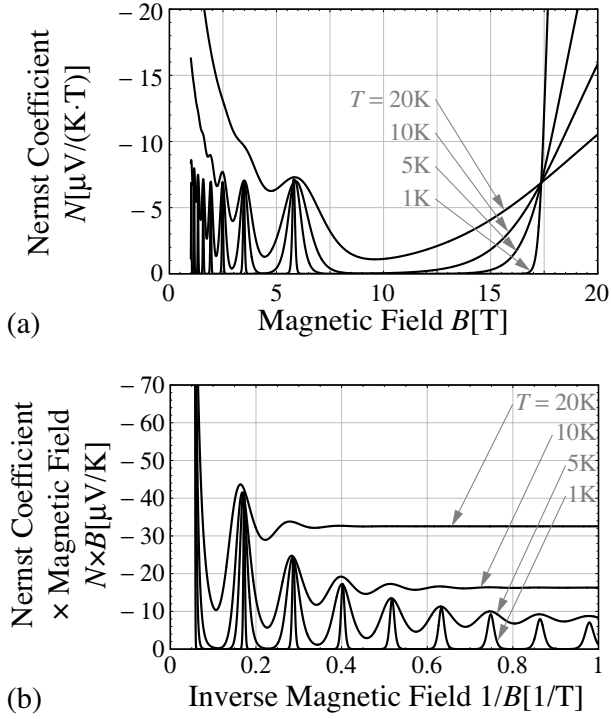
Fig. 4. The magnetic-field dependence of the adiabatic Nernst coefficient at $T = 1, 5, 10$ and 20K for $1\text{T} \leq B \leq 20\text{T}$; (a) the raw data and (b) a scaling plot of $N \times B$ against $1/B$.
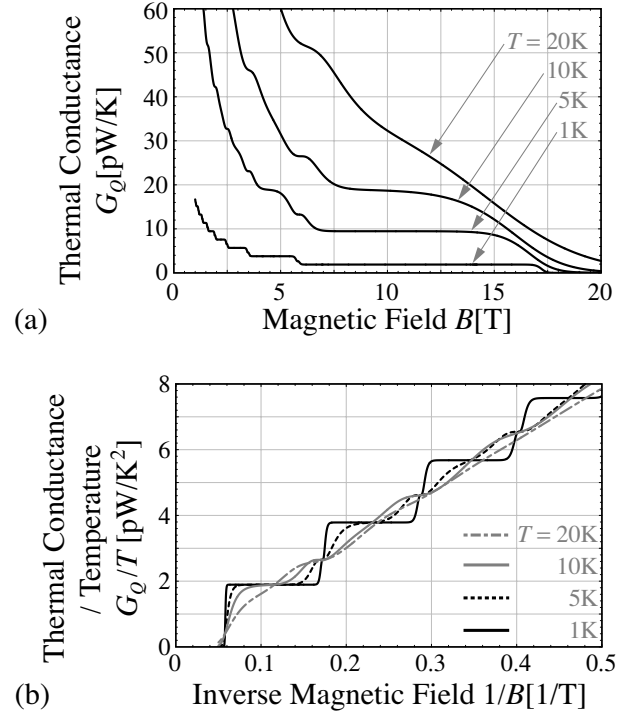

Fig. 5. The magnetic-field dependence of the thermal conductance at $T = 1, 5, 10$ and 20K for $1\text{T} \leq B \leq 20\text{T}$; (a) the raw data and (b) a scaling plot of G_Q/T against $1/B$.

Using these values, we obtained the adiabatic Nernst coefficient (16) as in Fig. 4 and the thermal conductance (17) as in Fig. 5. We see that our predictions are indeed realized at low temperatures. We also note that the Nernst coefficient is negative.

Summary: We predicted a prominent quantum effect in the Nernst coefficient and the thermal conductance of the two-dimensional electron gas, which is closely analogous to the quantum Hall effect. As long as the chemical potential stays in between the bottoms of the neighboring Landau levels, the quantized nature of the edge currents suppresses the Nernst coefficient and fixes the thermal conductance.

The precise forms of the peaks in Fig. 4 and the steps in Fig. 5 may be different from the reality. This is because our argument using the edge currents is not applicable when the chemical potential reaches the bottom of a Landau level, namely when $\mu = (n + \frac{1}{2})\hbar\omega_c$, or $1/B = (n + \frac{1}{2})\hbar|e|/m\mu$. There the heat current is carried by bulk states as well as the edge states. We then have to take account of impurities and possibly electron interactions.[12]

Comments on other approaches to the quantum Nernst effect are in order. Kontani derived[13,14] by the Fermi liquid theory general expressions of the thermoelectric power, the Nernst coefficient, and the thermal conductivity of strongly correlated electron systems such as high-T_c materials. Akera[15] analyzed the Ettingshausen effect, the reciprocal of the Nernst effect, by thermohydrodynamics. The quantum behavior predicted in the present paper, however, was not reported in either studies.

1) T. C. Harman and J. M. Honig: *Thermoelectric and Thermomagnetic Effects and Applications* (McGraw-Hill, New York, 1967) Chap. 7, p. 311.
2) S. Yamaguchi, A. Iiyoshi, O. Motojima, M. Okamoto, S. Sudo, M. Ohnishi, M. Onozuka, and C. Uesono: *Proc. 7th Int. Conf. Emerging Nuclear Energy Systems, Chiba, 1994* (World Scientific, Singapore, 1994) p. 502.
3) H. Nakamura, K. Ikeda, and S. Yamaguchi: Jpn. J. Appl. Phys. **38** (1999) 5745.
4) Y. Hasegawa, T. Komine, Y. Ishikawa, A. Suzuki, and H. Shirai: Jpn. J. Appl. Phys. **43** (2004) 35.
5) B. I. Halperin: Phys. Rev. B **25** (1982) 2185.
6) A. H. MacDonald and P. Středa: Phys. Rev. B **29** (1984) 1616.
7) S. Komiyama, H. Hirai, M. Ohsawa, Y. Matsuda, S. Sasa, and T. Fujii: Phys. Rev. B **45** (1992) 11085.
8) T. Martin and S. Feng: Phys. Rev. Lett. **64** (1990) 1971.
9) L. Smrcka, H. Havlova, and A. Isihara: J. Phys. C **19** (1986) L475.
10) K.-F. Berggren, T. J. Thornton, D. J. Newson, and M. Pepper: Phys. Rev. Lett. **57** (1986) 1769.
11) S. Tarucha, T. Saku, Y. Hirayama, and Y. Horikoshi: Phys. Rev. B **45** (1992) 13465.
12) H. Nakamura, N. Hatano, and R. Shirasaki: in preparation.
13) H. Kontani: Phys. Rev. Lett. **89** (2002) 237003.
14) H. Kontani: Phys. Rev. B **67** (2003) 014408.
15) H. Akera and H. Suzuura: cond-mat/0409498.